

Biparametric persistence for smooth filtrations

Mishal Assif P K¹, Yuliy Baryshnikov^{1,2,3}

¹University of Illinois, Department of ECE

²University of Illinois, Department of Mathematics

³Kyushu university, IMI

October 20, 2021

Abstract

The goal of this note is to define biparametric persistence diagrams for smooth generic mappings $h = (f, g) : M \rightarrow V \cong \mathbb{R}^2$ for smooth compact manifold M . Existing approaches to multivariate persistence are mostly centered on the workaround of absence of reasonable algebraic theories for quiver representations for lattices of rank 2 or higher, or similar artificial obstacles. We approach the problem from the Whitney theory perspective, similar to how single parameter persistence can be viewed through the lens of Morse theory.

1 Introduction

1.1 Persistence

We recall that the “classical”, one-parametric persistence deals with one parameter filtrations, an \mathbb{R} or \mathbb{Z} -indexed collection of subsets $\{X_s\}_{s \in I}$ of a topological space X such that $\cup_{s \in I} X_s = X$ and

$$X_s \subset X_t, \quad \text{if } s \leq t.$$

If $s \leq t$, the natural inclusions

$$i_{s,t} : X_s \rightarrow X_t$$

induce linear maps

$$(i_{s,t})_* : \mathbf{H}_k(X_s) \rightarrow \mathbf{H}_k(X_t)$$

(all homology groups here are over a field), so that satisfying the natural consistency (“functoriality”): for $r \leq s \leq t$

$$i_{s,t} \circ i_{r,s} = i_{r,t}.$$

This collection of vector spaces $\{\mathbf{H}_k(X_s)\}_{s \in I}$ connected by linear maps $\{(i_{s,t})_*\}_{s \leq t}$, is called the persistence module associated with the filtration.

One-parametric persistence theory asserts that upto isomorphism, this persistence module is completely characterized by a set of points in the plane called the persistence diagram [21]. Essentially, the whole collection of homology mappings split into chains of isomorphisms, whose terminal points, - birth and death points, - carry a lot of information about the filtration.

This theory, appearing in different guises essentially since Morse work, provided an essential toolbox for many researchers dealing with filtrations, from geometric analysis to data analysis.

The authors were supported by the ARO through the MURI ‘Science of Embodied Innovation, Learning and Control’.

The diagrams of birth-death pairs, known as the *persistence diagrams* are known to be stable with respect to perturbations in a certain sense [7], and can be computed algorithmically [8].

Biparametric persistence deals with the filtrations indexed by points in the plane, \mathbb{R}^2 or \mathbb{Z}^2 endowed with the usual product order relation.

1.1.1 Slices and Bipersistence

In the smooth category, the following definition is natural.

Let $h = (f, g) : M \rightarrow \mathcal{V} \cong \mathbb{R}^2$ be a map from the topological space M to the plane. We define the $c = (a, b)$ -*slice* of a manifold as the set

$$M_c = M_{a,b} = \{f \leq a, g \leq b\}.$$

We also denote the sublevel sets of f and g as

$$F_a = \{f \leq a\}, \quad G_b = \{g \leq b\}.$$

We say $c_1 = (a_1, b_1) \prec c_2 = (a_2, b_2)$ when

$$a_1 \leq a_2, \quad b_1 \leq b_2.$$

The sublevel sets $\{F_a\}_{a \in \mathbb{R}}$ form a one-parameter filtration of M , while the slices $\{M_c\}_{c \in \mathbb{R}^2}$ give rise to a biparametric filtration on M . The persistence module associated with such bi-filtrations are the central object of our study.

1.2 Context: Biparametric Persistence

The goal of this note is to define the biparametric persistence diagrams for smooth generic mappings $h = (f, g) : M \rightarrow \mathcal{V} \cong \mathbb{R}^2$ for smooth compact manifold M .

Existing approaches to multivariate persistence are mostly centered on the workaround of absence of reasonable algebraic theories for quiver representations for lattices of rank 2 or higher, or similar artificial obstacles, and thus are focused on the discrete filtrations [11, 13–15].

An alternative thread of research dealing with the biparametric persistence relies on restricting the filtration to straight lines with a positive slope in the plane of parameters, and studying the resulting (two-parametric) family of one-parametric persistence diagram, see [4–6].

There are other treatises of biparametric persistence, exploring the space adjacent to the major threads we mentioned, see e.g. [17, 19].

Our view on the problem was driven by the parallels between the Morse theory and persistence theory: the latter is a subtle globalization of the former. The corresponding singularity theory for the biparametric persistence theory would deal with the critical points of smooth mappings into \mathbb{R}^2 , a classical topic, going back to H. Whitney [20]. What is the persistence theory for such mappings? This was the primary motivating question guiding this research.

Another guiding idea was to dramatically expand the (natural) approach of describing the persistence structures on the increasing one-parametric filtrations induced from the biparametric ones. To this end we replace the family of straight lines with positive slopes deployed by Frosini and his co-authors to the functional family of arbitrary increasing curves. While the resulting family of curve is infinite dimensional, this approach allows one to keep track of all patterns of the biparametric filtrations. Moreover, the space of increasing curves can be effectively discretized, leading to a finite (for compact source manifold) cubical $\text{CAT}(0)$ complex [16] with the one-dimensional persistence data attached to its vertices, giving a complete description of the biparametric diagram.

1.3 Singularities of mappings into the plane

Recall that Morse theory asserts that a generic real valued function on a compact manifold has its critical points nondegenerate, isolated, and having different critical values. In addition, the

local form of such a function in a neighborhood of its critical point is completely determined by a single integer, called the index, associated with each critical point. This gives significant information about the evolution of topology of the slice sets of such a function.

Whitney theory [20] parallels Morse theory for the mappings into the plane, and we will use it to understand the evolution of the homology of the slice sets.

Definition 1.1. *Singular set $\Sigma(h) \subset M$ of h is the set of points $x \in M$ where the rank of the Jacobian $D_x h : T_x M \rightarrow \mathbb{R}^2$ is less than maximal (i.e. less than 2).*

The image $h(\Sigma(h))$ is called the visible contour of h .

Whitney established that for a generic map (i.e. a map belonging to an open dense subset of smooth maps), the rank of the Jacobian does not drop to zero, and the singular set is a smooth curve in M . Moreover, at the singular points, an appropriate choice of coordinates in M and V brings h to one of the two canonical forms:

1. $f(x_1, \dots, x_m) = x_1, \quad g(x_1, \dots, x_m) = q(x_2, \dots, x_m),$
2. $f(x_1, \dots, x_m) = x_1, \quad g(x_1, \dots, x_m) = x_2^2 + x_1 x_2 + q(x_3, \dots, x_m),$

where q is a non-degenerate quadratic function. The points of the first kind are called the *fold points*, and h restricted to $\Sigma(h)$ is an immersion at such points.

The points of the second type are isolated (and therefore, there is only finitely many of them, as M is compact). Such points are called *cusp points* which are characterized by the fact that the Jacobian of h restricted to $\Sigma(h)$ degenerates.

Therefore h is an immersion of $\Sigma(h)$ at the fold points (so its image is a smooth curve, perhaps with self-intersections), and the cusp points map to cusps on the visible contour.

Definition 1.2. *The h -images of critical points of f are called vertical, of g , horizontal points.*

Applying the standard arguments (see, e.g. [9]) leads to the following

Proposition 1.3. *For generic h the set of critical points $\Sigma(h)$ is a smooth curve in M , mapping to a curve with cusps and simple self-intersections in V , and the component functions f, g are Morse, with the critical points distinct from the cusp points, and map to different points by h .*

Further, the tangents to the h -image of the fold points is vertical or horizontal exactly at the vertical or horizontal points, the curvatures of the visible contour at the critical points of f and g are non-vanishing, and the the points of the self-intersection of the fold curve are neither horizontal nor vertical.

As the rank of the Jacobian is 1 at the fold points, there is a unique (up to a multiple) linear combination of the differentials of f and g vanishing there. If the coefficients are of the same sign, we will say that the point has *negative slope*, otherwise, *positive slope*.

The nonvanishing of the curvature of the contour at the fold points (in particular, at the vertical and horizontal points) established for the generic maps implies that vertical and horizontal points split the fold curve into a finite number of the alternating segments of positive and negative slope points.

2 Pareto Grid

2.1 Pareto Points and Extension Rays

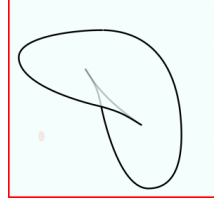
Previous applications of the Whitney theory dealt with the simultaneous optimization of several functions (important in economic theory), see e.g. [18], motivating the following nomenclature:

Definition 2.1. *The (closure) of contour points of negative slope is called the set of Pareto points: they form a collection of curves with cusps and self-intersections with boundaries at horizontal and vertical points.*

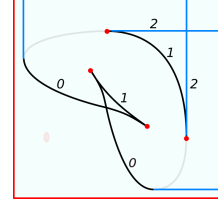
Augment the set of Pareto points with the union of vertical and horizontal rays, attached to the (correspondingly) vertical and horizontal points, and such that the respective coordinate increases to $+\infty$ along the ray.



(a) Chicago Millenium Park



(b) Visible contour



(c) Pareto grid

Figure 1: Figure (a) shows a bean sculpture, the surface of which is a 2 dimensional sphere. If h is the projection of the surface onto a plane behind the bean the corresponding visible contour is shown in Figure (b). The Pareto grid, along with cusps, pseudocusps and indices of various segments of the grid are shown in Figure (c).

Definition 2.2. We will be referring to such rays as the extension rays, and the union of Pareto segments and the extension rays in the (f, g) plane as the Pareto grid.

(We borrowed the term *Pareto grid* from [5], who introduced this notion independently in 2019.)

Definition 2.3. A boundary point of a Pareto segment is called a pseudocusp if the extension ray does not attach smoothly with the Pareto segment at the point.

An illustration of all these definitions is given in Figure 1. The Pareto grid shown on the right display has two cusps and two pseudocusps indicated as points in red. The blue lines are the extension rays and the black curves are the Pareto segments. There is one vertical and one horizontal point on the Pareto grid which are not pseudocusps as the extension rays at these points fit smoothly with the Pareto segment.

2.2 Topology of Slices

In biparametric persistence, the Pareto grid plays a role analogous to set of critical values of a Morse function in one-parametric persistence theory. Outside of it, the topology of the slices does not change, and across it, it changes in a controllable way.

Theorem 2.4. The slices M_c are homeomorphic as c varies within an (open) connected component of the complement to the Pareto grid.

Crossing the Pareto grid leads to easy to interpret changes in the topology of the slices.

Theorem 2.5. For each pair of ordered points in V , such that a path connecting them intersects the Pareto grid transversally at a single point which is not a cusp or a pseudo-cusp, the higher slice is homotopy equivalent to the lower one with a single cell of dimension k attached by its boundary.

Proof of Theorem 2.4. We need to prove that M_c is homeomorphic to $M_{c'}$ for c' close enough to c . It is clearly enough to prove that for c' differing from c just in one coordinate: say, $c = (a, b)$; $c' = (a', b)$. By definition, the hypersurfaces $\{f = a\}$ and $\{g = b\}$ in M are smooth, and intersect transversally near the slice M_c . Now, the result follows immediately from collaring theorems for the manifolds with boundaries and submanifolds intersecting them transversally (see, e.g. [12]). \square

Proof of Theorem 2.5. Let c be a point of the Pareto grid which is not a (pseudo)-cusp. As in the proof of Theorem 2.5, it is enough to consider a pair of points close to $c = (a, b)$ that differ from c only in one coordinate, say $a' < a < a''$. In this case we consider the change in topology of the sublevel set of a Morse function f on the manifold with boundary given by $G_b = \{g \leq b\}$. This is, of course, a well-established subject, see e.g. [2, 10].

We need to distinguish two cases:

- If a is the critical value of f corresponding to a critical point x in the interior of G_b , the point c is located on the extension ray. In this case, the claim follows immediately, as by the assumptions, f is a Morse function, and all local changes of the topology near x amount to attaching a cell of the dimension equal to the index of f at x . (Outside of some vicinity of x , the collaring theorem applies again.)
- If a is the critical value of the restriction of f to the boundary $\{g = b\}$ of G_b , then, again by genericity, the corresponding critical point x is Morse, and we are locally dealing with, in an appropriate chart with the with the change of topology of the sets

$$M_\alpha := x_1 \geq 0; x_1 \leq \phi(x_2, \dots, x_m) + \alpha$$

as α varies across 0, and ϕ is a Morse function (of the same index k as the restriction of f to G_b at x). It is immediate, that locally, the change of topology amounts to addition of a cell of index k .

This proves the result. □

2.3 Indices on the Grid

The results of the previous section allow us to attach indices to the component curves of the Pareto grid.

Definition 2.6. *We will refer to the dimension k of the cell attached when crossing a point on the Pareto grid as the index of the point.*

It is equal, to remind, to the index of f or g at the critical point corresponding to an extension ray, and to the index of the restriction of one of the functions to the level set of the other, for the Pareto points of the grid.

It is known that attaching a k -cell to a space has the effect of either increasing the dimension of \mathbf{H}_k by one or decreasing that of \mathbf{H}_{k-1} by one. This can be phrased algebraically as

1. $(i_{\gamma(a), \gamma(b)})_* : \mathbf{H}_k(M_{\gamma(a)}) \rightarrow \mathbf{H}_k(M_{\gamma(b)})$ is injective with cokernel of dimension 1,
2. $(i_{\gamma(a), \gamma(b)})_* : \mathbf{H}_{k-1}(M_{\gamma(a)}) \rightarrow \mathbf{H}_{k-1}(M_{\gamma(b)})$ is surjective with kernel of dimension 1.

This implies, inter alia, that the index is constant along the segments of the Pareto grid outside of cusps or pseudo-cusps:

Proposition 2.7. *The dimensions of the attached cells are constant along the smooth immersed components of the Pareto grid, the complements to the (pseudo)cusps.*

Proof. Consider first the smooth components of the Pareto grid away from the cusps or pseudocusps. We know (by Theorem 2.4 that the topology is constant on either side of that smooth curve. Hence, the changes of the topology should be the same wherever on crosses it.

The situation near the intersecting components of the Pareto grid is also clear: the changes of the topology caused by the crossing of either of the components are localized near the corresponding critical points, which are distinct, and therefore are independent of each other. □

Another implication of the Proposition 2.7 allows us to characterize the indices of the branches of the Pareto grid connecting at a (pseudo) cusp: the change in index of a smooth segment of the Pareto grid at a (pseudo) cusp is also characterized in the following result.

Proposition 2.8. *At the (pseudo)cusps, the points of the two branches are naturally ordered: any point of one branch near the (pseudo) cusp is greater than (some of the) points of the other (we will call the former branch the upper, the latter, the lower one). The index of the upper branch exceeds the index of the lower branch by one.*

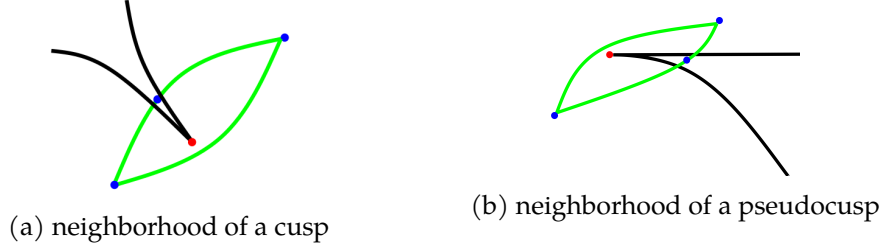


Figure 2: Curves in a neighborhood of a (pseudo)cusp.

Proof. Consider a pair of points outside of the Pareto grid, one slightly above, one slightly below the cusp. As they belong to the same connected component of the complement to the Pareto grid, the corresponding slices are homeomorphic. On the other hand, one can find an increasing curve connecting these two points, intersecting the Pareto grid at two branches joined at the cusp. At each of the branches a disk of some dimension is attached to the slice, resulting in trivial change of the topology. By inspection, this is possible only if at the upper branch, the class generated by the lower one was annihilated, implying the result. \square

3 Increasing curves and persistence

We will be referring to the pseudocusps and cusps as *obstacles*. Consider an *increasing curve* $\gamma : \mathbb{R} \rightarrow \mathbb{R}^2$ in the f, g -plane (this means that both functions strictly increase along the curve). To fix the gauge, we will assume that the curve is parameterized by $f + g$ (we will refer to this parameter as the *natural height*).

An increasing curve γ defines a usual I-indexed filtration of M , and correspondingly, persistent homologies and persistent diagrams $\mathbf{PH}_k(\gamma), k = 0, \dots, m$, which we interpret as a collection of distinguishable points in planes $\{b < d\}$. The results of the previous section describe the nature of these persistence diagrams. When the curve hits an index k segment of the Pareto grid, a k -cell is attached to the slice set and so either the dimension of the k -th homology of the slice set increases by one or that of the $k - 1$ -th homology decreases by one. Therefore certain pairs of intersections of the curve γ with an index k segment and an index $k + 1$ segment leads to a birth-death pair in the k -th homology of the slice set, and such pairs collected together form the persistence diagram $\mathbf{PH}_k(\gamma)$.

Remark 3.1. *The approach to multiparametric persistence through restriction to increasing straight lines has been considered by [5, 13].*

We will see that we can completely describe the change in persistence diagram as the curve varies in the set of increasing curves with fixed endpoints avoiding the obstacle points. It is natural to understand this space of increasing curves first.

Proposition 3.2. *In a generic family of increasing paths (and for a generic \mathfrak{h}), the sets of paths passing through an obstacle is a smooth hypersurface; the hypersurfaces corresponding to the different obstacles intersect transversally.*

The hypersurfaces are naturally cooriented (by the increase of number of intersections with the Pareto grid).

We say that increasing curves γ and γ' connecting the same endpoints belong to the same path-connected collection if there exists a homotopy of increasing curves fixing the endpoints connecting the two curves. The following sequence of results describe how the persistent homology changes as the curve γ moves in the space of increasing paths.

Theorem 3.3. *For the path-connected collection of increasing curves in the plane avoiding obstacles, there is a section of the space of persistent diagrams: that is for any two such curves γ, γ' , there is an*

identification

$$I(\gamma', \gamma) : \mathbf{PH}_*(\gamma) \rightarrow \mathbf{PH}_*(\gamma'),$$

of the bars in the persistent diagrams corresponding to each of the curves, and these identifications are consistent:

$$I(\gamma'', \gamma')I(\gamma', \gamma) = I(\gamma'', \gamma).$$

Proof. We denote by $PG \supset PG_k \supset PG_k^\gamma$ the set of smooth segments of the complement of obstacles of the Pareto grid, the set of smooth segments of index k and the set of smooth segments of index k and hitting the increasing curve γ respectively. If $l \in PG_k^\gamma$, we will denote by t_l^γ the unique time at which γ hits l .

If γ and γ' satisfy the conditions of the theorem, $PG_k^\gamma = PG_k^{\gamma'}$ for all k . Only when a curve crosses either a pseudocusp or a cusp can it hit a new segment of the Pareto grid.

As far as \mathbf{PH}_k is concerned, only the index k and $k + 1$ segments matter. So we prove this result in three stages, assuming the curves γ and γ' can be connected to each other by a homotopy

1. avoiding the obstacles and intersection points of two segments from $PG_k \cup PG_{k+1}$,
2. avoiding the obstacles and intersection points of two segments of the same index,
3. avoiding the obstacles only.

Case 1: In this case, it is not only true that $l \in PG_k^\gamma = PG_k^{\gamma'}$ but the order in which the two curves hit each smooth segment is also the same. The recipe to construct the identification $I_k(\gamma', \gamma)$ between the persistence diagrams of γ and γ' is to simply map $(t_{l_1}^\gamma, t_{l_2}^\gamma) \in \mathbf{PH}_k(\gamma)$ to $(t_{l_1}^{\gamma'}, t_{l_2}^{\gamma'}) \in \mathbf{PH}_k(\gamma')$. The consistency of this identification follows obviously. We just need to show that $(t_{l_1}^\gamma, t_{l_2}^\gamma) \in \mathbf{PH}_k(\gamma) \implies (t_{l_1}^{\gamma'}, t_{l_2}^{\gamma'}) \in \mathbf{PH}_k(\gamma')$.

We show this assuming γ' lies in an ϵ tube around γ for small enough ϵ . The general result will follow since γ and γ' can be connected by finitely many such tubes. If the ϵ is small enough, we can choose points $\gamma(t_{i_i}^\pm)$ just after and before $\gamma(t_{i_i})$ for $i = 1, 2$. We can do the same for γ' , and then choose c_i^- close to $\gamma(t_{i_i})$ such that $c_i^- \prec \gamma(t_{i_i}^-)$ and $c_i^- \prec \gamma'(t_{i_i}^-)$, and a c_i^+ also close to $\gamma(t_{i_i})$ such that $c_i^+ \succ \gamma(t_{i_i}^+)$ and $c_i^+ \succ \gamma'(t_{i_i}^+)$. These choices are illustrated in Figure 3. If ϵ is close enough, the inclusions $i_{c_i^-, \gamma_{t_i}^-}, i_{c_i^-, \gamma'_{t_i}^-}, i_{\gamma_{t_i}^+, c_i^+}, i_{\gamma'_{t_i}^+, c_i^+}$ are all homotopy equivalences.

The existence of a bar between t_{l_i} and t_{l_j} along γ is equivalent to the existence a homology class α in $\mathbf{H}_k(M_{\gamma(t_{i_i}^+)})$ that is:

- (i) not in the image of $i_{\gamma(t_{i_i}^-), \gamma(t_{i_i}^+)}$,
- (ii) whose image under $i_{\gamma(t_{i_i}^+), \gamma(t_{i_j}^-)}$ is not in the image of $i_{\gamma(t_{i_i}^-), \gamma(t_{i_j}^-)}$,
- (iii) and whose image under $i_{\gamma(t_{i_i}^+), \gamma(t_{i_j}^+)}$ is in the image of $i_{\gamma(t_{i_i}^-), \gamma(t_{i_j}^+)}$.

We can push this class α via the isomorphism $i_{\gamma(t_{i_i}^+), c_i^+}$ to obtain a homology class that is:

- (i) not in the image of $i_{c_i^-, c_i^+}$,
- (ii) whose image under $i_{c_i^+, c_j^-}$ is not in the image of $i_{c_i^-, c_j^-}$,
- (iii) and whose image under $i_{c_i^+, c_j^+}$ is in the image of $i_{c_i^-, c_j^+}$,

owing to the fact that each $c_{i/j}^\pm$ point and the corresponding $t_{i/j}^\pm$ point has been chosen such that inclusion induces an isomorphism in the k -th homology between them. This same procedure can be used to push this class onto the corresponding $t_{i/j}^\pm$ points to obtain a homology class that is born at $t_{i_i}^+$ and dies at $t_{i_j}^+$ along γ' . This proves the result for case 1.

Case 2: In this case, there can be intersections between an index k and an index $k + 1$ segment of the grid. This situation is illustrated in Figure 4. We have two segments l_l, l_r of the Pareto grid intersecting at a point. We can also just show the result for curves γ and γ' that are equal outside a neighborhood of the intersection point. Suppose l_l has index k and l_r has index $k + 1$.

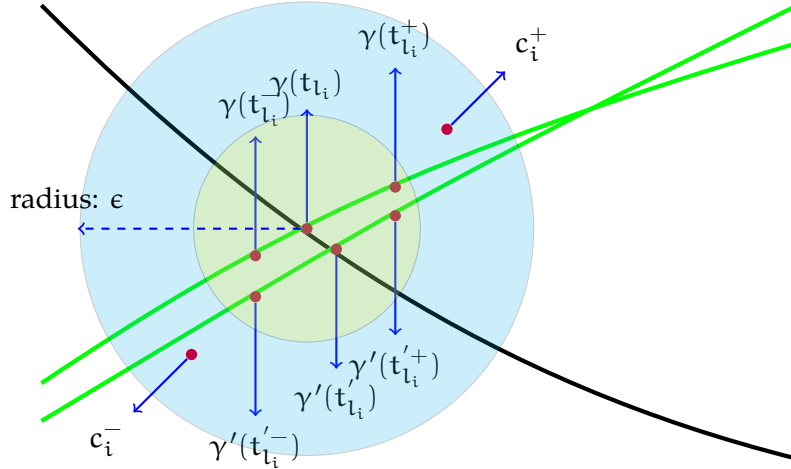


Figure 3: The green increasing lines indicate the curves γ and γ' and the black line with negative slope is the piece of the life contour l . The blue disk around $\gamma(t_{l_i})$ is a possible choice for the ϵ tube. Also indicated are possible choices for $t_{l_i}^{\pm}, t_{l_i}'^{\pm}, c_i^{\pm}$.

The same mapping in case 1, sending $(t_{l_1}^{\gamma}, t_{l_2}^{\gamma}) \in PH_k(\gamma)$ to $(t_{l_1}^{\gamma'}, t_{l_2}^{\gamma'}) \in PH_k(\gamma')$ will work in this case as well. All that needs to be shown is that a bar born along l_1^- will not die at l_1^- . If this did happen,

$$i_{c^-, \gamma(t^+)} \circ i_{\gamma(t^-), c^-} = i_{\gamma(t^-), \gamma(t^+)}$$

would be an isomorphism. However,

$$i_{c^+, \gamma(t^+)} \circ i_{\gamma(t^-), c^+} = i_{\gamma(t^-), \gamma(t^+)}$$

can't be an isomorphism, as $i_{\gamma(t^-), c^+}$ is not injective.

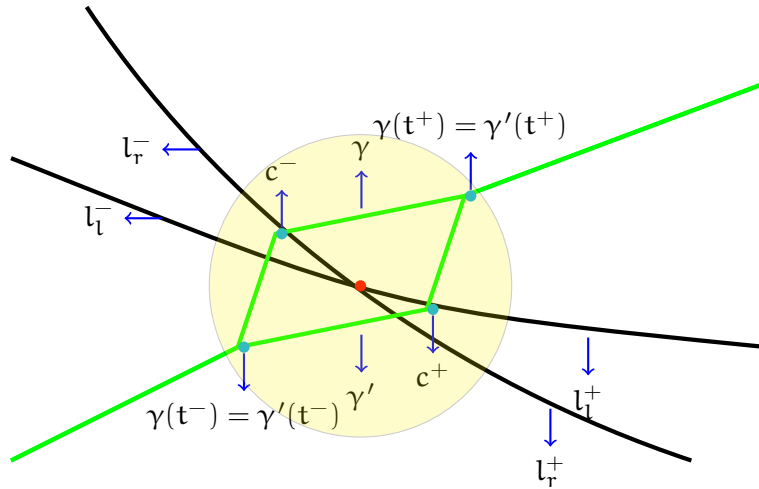


Figure 4: The green increasing lines indicate the curves γ and γ' and the black lines with negative slope are two segments of the Pareto grid. The figure indicates the further splitting of the two segments into four pieces by the intersection point.

Case 3: In this final case, we have to consider intersections of segments of the same index k as well. Figure 4 serves as an illustration for this case as well, with the difference that l_l

and l_τ both have index k . The usual mapping employed in the earlier cases won't necessarily work here. For instance, if l_l^- cause the birth of a cycle while l_r^- causes a death, it could be the case that l_l^+ causes a death while l_r^+ causes a birth. In such situations where the bars flip at a double point of the same index, we need to augment the incident segments of the life contour by connecting l_l^- with l_r^+ and l_r^- with l_l^+ . After this possible augmentation, the earlier map between persistence diagrams work here as well. \square

The following proposition clearly follows from the above proof.

Proposition 3.4. *If the deformation of the increasing curve avoids not just the obstacles, but also the double points of the Pareto grid where the branches of the same index intersect, then the chains representing the elements of each of the persistent homology groups can be transported, consistently, along the deformation.*

As the increasing path crosses a double point of the Pareto grid, the persistent diagram changes continuously, but the birth or death times of a pair of cycles cross, and their corresponding cycles can flip. This phenomenon was noted in [5]. In some sense, this implies that one cannot observe the *Elder Rule* [8] functorially along the increasing curve in biparametric persistence.

We can also predict what happens when the curve crosses an obstacle.

Proposition 3.5. *The increasing curve crossing into (out of) a region with higher number of intersections with the Pareto grid leads to the birth (death) of a k -dimensional persistence bar at the the natural height of the corresponding (pseudo) cusp.*

Proof. The proof of the result follows from the proof of 2.8. Figure 2 shows the neighborhood of an obstacle. Crossing an obstacle into the region where the curve intersects more with the Pareto grid clearly leads to the creation of a k -bar across the adjacent segments of the grid. \square

Remark 3.6. *After the augmentation possibly required at double points of the same index, the collection of augmented segments of the Pareto grid get paired together as lines of negative slope meeting at obstacles, across which homology cycles are born and killed. A pair of such curves, with index k and $k+1$, contains a region B^k enclosed between them. The set of these regions $\{B_i^k\}$ are analogous to the barcodes in single parameter persistent homology; given points $c_1 \prec c_2 \in V$,*

$$\mathrm{rk} \left((i_{c_1, c_2})_* : \mathbf{H}_k(M_{c_1}) \rightarrow \mathbf{H}_k(M_{c_2}) \right) = \#\{B_i^k \mid c_1, c_2 \in B_i^k\}$$

4 Space of Obstacle Avoiding Curves

The result of the previous section forces us to concentrate on the spaces of the increasing curves avoiding obstacles: as we established, any two such curves which can be homotoped one into another avoiding obstacles define functorially equivalent persistence diagrams. Therefore, it is important to understand the structure of the components of obstacle avoiding increasing curves.

4.1 Components of the Obstacle Avoiding Curves

The problem of enumeration of these components turned out to be remarkably simple.

Proposition 4.1. *The connected components of a space of increasing curves in the plane avoiding a finite set of obstacles $o_1, \dots, o_k \in \mathbb{R}^2$ are contractible, and their number is equal to the number of chains of obstacles, i.e. subsets $o_{i_1} \prec \dots \prec o_{i_n}$, where $o_m \prec o_n$ is the vector ordering of the points (empty chain included).*

Proof. By turning the V plane by 45° , we can identify the increasing paths with the (strictly) Lipschitz functions with constant $L = 1$. Consider the decomposition of such functions avoiding the obstacles into open components: they are obviously convex.

For any such component, the pointwise infimum of all trajectories in it (recall that we identify the trajectories with Lipschitz functions $x : [0, T] \rightarrow \mathbb{R}$) is a Lipschitz function passing through some collection of obstacles. Those of the obstacles where x_γ is not locally linear necessarily form a chain, which we will refer to as the *marker* of the component. This gives a mapping from the components of the space of obstacle avoiding paths to the chains of obstacles.

To reverse the correspondence, i.e. to associate to a chain a component, pick a small slack ϵ , and for a chain γ consider the function

$$x_\gamma(t) := \max_{k \in \gamma} (x_k + \epsilon - (1 - \epsilon)|t - t_k|).$$

One can easily see that for small enough ϵ , this function will be in the component whose marker coincides with the chosen chain. This bijection proves the statement. \square

This correspondence is illustrated in Figure 5.

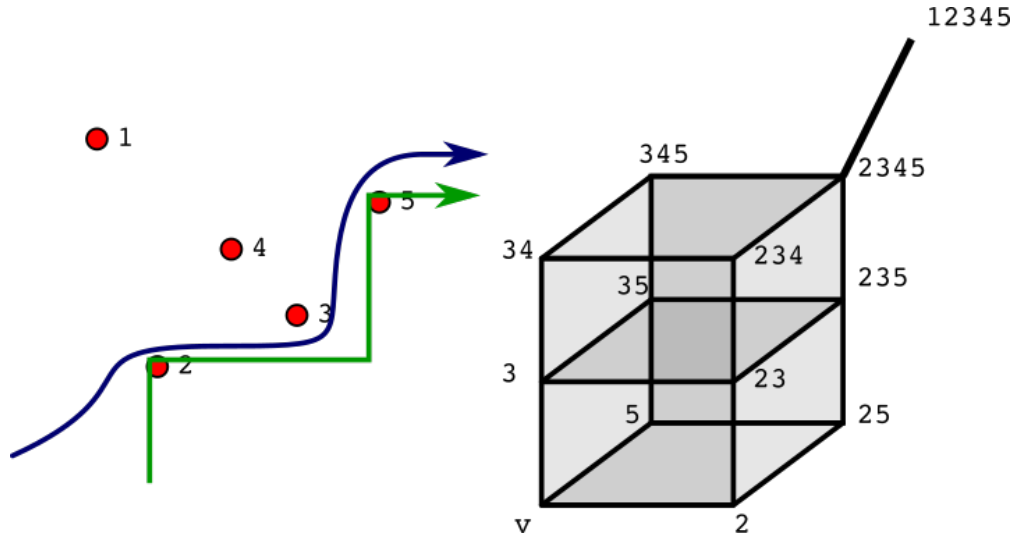


Figure 5: Left display: curves avoiding obstacles and their corresponding chains. The red points are obstacles. The blue curve has the marker shown in green, corresponding to the chain $o_2 \prec o_5$.

Right display: cubical complex corresponding to the obstacles on the left display. See Section 4.2 for the explanation of the labels.

4.2 Cubical Complexes

From our structural theorems about the behavior of the persistence diagrams along the increasing paths as the paths cross the obstacles (i.e. cusps or pseudocusps), it is clear that the adjacency of the components of the space of increasing paths is of interest on its own right. Indeed, crossing an obstacle generates or kills a bar on the persistence diagram, and so one can algorithmically generate the persistence diagrams basing on the adjacencies of the components (and the natural heights of the points of the intersection of the increasing curves with the Pareto diagram).

In the space of increasing curves (which we assume throughout to be parameterized by their natural height, and thus equivalent to the space of $L = 1$ Lipschitz functions), the condition of passing through an obstacle forms a codimension 1 hyperplane.

The following is quite obvious:

Proposition 4.2. *The multiple intersections of the hyperplanes corresponding to the obstacles are transversal, and contractible.*

Proof. The transversality follows immediately from the definition; the contractibility from the fact that each component of the set of the increasing curves passing through a given collection of obstacles and avoiding any other obstacle, is convex, if interpreted as functions of the natural height. \square

Consider the cellular complex dual to the space the increasing curves, stratified by the obstacles they pass through. Each of the components becomes a vertex, adjacent cells become connected by an edge etc. The transversality of the intersection implies that the resulting cellular complex is *cubical*, that is obtained by the dimension preserving identifications of cubical facets of various cubes.

Definition 4.3. *We will refer to the complex dual to the stratification of the space of increasing curves by the obstacles they pass through as the obstacle complex.*

A class of cubical complexes found an extensive use in geometric group theory: namely, the complexes of non-positive curvature (one can turn cubical complexes into path metric spaces by considering flat metric on each of them, in which they are rectangular parallelepipeds (still to be referred to as cubes) whose identified sides have equal lengths). One refers to such metric spaces as CAT(0) ones, if they satisfy the classical comparison bounds, see [3]. It is well known that a cubical space has non-positive curvature if Gromov's condition is satisfied: in the link of any cube, any three adjacent cubes each sharing a facet will be facets of a common cube, - in other words, nonpositive curvature of a cubical complex depends only on the combinatorial data. A simply-connected cubical complex of nonpositive curvature is referred to as a *cubing* (for the details and origins of the nomenclature, see [16]).

Proposition 4.4. *The obstacle complex is a cubing.*

Proof. The only non-immediate fact requiring verification is Gromov's condition, which amounts to the following statement: if for some three obstacles on the plane, there are increasing paths going through each pair of them, then there is a path going through all three. Ordering the obstacles by their natural height makes that obvious. \square

The cubes of the obstacle complex, as established, correspond to the chains of obstacles, and the dimension of the cubing, - i.e. the highest dimension of the constituent cubes, - equals the length of the longest chain of obstacles. Right display of the Figure 5 shows the cubing corresponding to the obstacle configuration on the left. We use the convention of [1] to mark vertices of the cubing (i.e. increasing obstacle avoiding paths); as one can see (and prove with ease), the markings to markers as defined in Proposition 4.1.

The configuration of obstacles equips the rectangular parallelepipeds ("cubes") of a cubing with natural edge lengths (the smallest of the increments of coordinates between two ordered obstacles in the corresponding chain chain). Continuous deformations of the configurations of obstacles leads to continuous deformation of thus metrized cubing (the distance between which is defined using the Gromov-Hausdorff metric). It seems quite plausible that the function associating such a metric cubings to a smooth map from a manifold to the plane is continuous, providing a version of biparametric stability.

5 Concluding Discussion

This note represents just an introduction to the notion of biparametric persistence via increasing paths. We plan to return to the topic addressing some of the results conjectured here (such as stability), and generalizations (to the manifolds with boundary or corners).

References

- [1] Federico Ardila, Megan Owen, and Seth Sullivant. Geodesics in CAT(0) cubical complexes. *Advances in Applied Mathematics*, 48(1):142–163, January 2012.

- [2] V. I. Arnol'd. Wave front evolution and equivariant Morse lemma. *Communications on Pure and Applied Mathematics*, 29(6):557–582, 1976.
- [3] Martin R Bridson and André Haefliger. *Metric spaces of non-positive curvature*, volume 319. Springer Science & Business Media, 2013.
- [4] Andrea Cerri, Barbara Di Fabio, Massimo Ferri, Patrizio Frosini, and Claudia Landi. Multidimensional persistent homology is stable. *arXiv:0908.0064 [math]*, August 2009. arXiv: 0908.0064.
- [5] Andrea Cerri, Marc Ethier, and Patrizio Frosini. On the geometrical properties of the coherent matching distance in 2d persistent homology. *Journal of Applied and Computational Topology*, 3(4):381–422, Dec 2019.
- [6] Andrea Cerri and Patrizio Frosini. Necessary conditions for discontinuities of multidimensional persistent betti numbers. *Mathematical methods in the applied sciences*, 38(4):617–629, 2015.
- [7] David Cohen-Steiner, Herbert Edelsbrunner, and John Harer. Stability of persistence diagrams. *Discrete & computational geometry*, 37(1):103–120, 2007.
- [8] Herbert Edelsbrunner and John Harer. *Computational topology: an introduction*. American Mathematical Soc., 2010.
- [9] M. Golubitsky and V. Guillemin. *Stable mappings and their singularities*. Graduate Texts in Mathematics, Vol. 14. Springer-Verlag, New York-Heidelberg, 1973.
- [10] Mark Goresky and Robert MacPherson. *Stratified Morse Theory*. Springer Berlin Heidelberg, Berlin, Heidelberg, 1988. OCLC: 851730539.
- [11] Heather A. Harrington, Nina Otter, Hal Schenck, and Ulrike Tillmann. Stratifying multiparameter persistent homology. *SIAM J. Appl. Algebra Geom.*, 3(3):439–471, 2019.
- [12] Morris W Hirsch. *Differential topology*, volume 33. Springer Science & Business Media, 2012.
- [13] Michael Lesnick. The theory of the interleaving distance on multidimensional persistence modules. *Found. Comput. Math.*, 15(3):613–650, 2015.
- [14] Michael Lesnick and Matthew Wright. Computing Minimal Presentations and Betti Numbers of 2-Parameter Persistent Homology. *arXiv preprint arXiv:1902.05708*, 2019.
- [15] Ezra Miller. Data structures for real multiparameter persistence modules. *arXiv preprint arXiv:1709.08155*, page 107, 2017.
- [16] Michah Sageev. Ends of Group Pairs and Non-Positively Curved Cube Complexes. *Proceedings of the London Mathematical Society*, 3(71), 1995.
- [17] Sara Scaramuccia, Federico Iuricich, Leila De Floriani, and Claudia Landi. Computing multiparameter persistent homology through a discrete morse-based approach. *Computational Geometry*, 89:101623, 2020.
- [18] Steve Smale. Global analysis and economics. *Synthese*, 31(2):345–358, August 1975.
- [19] Oliver Vipond. Multiparameter Persistence Landscapes. page 38.
- [20] Hassler Whitney. On singularities of mappings of euclidean spaces. i. mappings of the plane into the plane. *Annals of Mathematics*, 62(3):374–410, 1955.
- [21] Afra Zomorodian and Gunnar Carlsson. Computing persistent homology. *Discrete & Computational Geometry*, 33(2):249–274, 2005.